Advanced Synthesis & Catalysis

Accepted Article

Title: Efficient Synthesis of 12-Oxochenodeoxycholic Acid Using a 12α-Hydroxysteroid Dehydrogenase from Rhodococcus ruber

Authors: Shou-Cheng Shi, Zhi-Neng You, Ke Zhou, Qi Chen, Jiang Pan, Xiao-Long Qian, Jian-He Xu, and Chun-Xiu Li

To be cited as: *Adv. Synth. Catal.* 10.1002/adsc.201900849

Link to VoR: http://dx.doi.org/10.1002/adsc.201900849

VERY IMPORTANT PUBLICATION COMMUNICATION

DOI: 10.1002/adsc.201((will be filled in by the editorial staff))

Efficient Synthesis of 12-Oxochenodeoxycholic Acid Using a 12α-Hydroxysteroid Dehydrogenase from *Rhodococcus ruber*

Shou-Cheng Shi,[a, #] Zhi-Neng You,[a, #] Ke Zhou,[a] Qi Chen,[a, b] Jiang Pan,[a, b] Xiao-Long Qian,[c] Jian-He Xu,[a, b, *] and Chun-Xiu Li [a, b, *]

[a] Laboratory of Biocatalysis and Synthetic Biotechnology, State Key Laboratory of Bioreactor Engineering, East China University of Science and Technology, 130 Meilong Road, Shanghai 200237, P. R. China
Fax: (+86)-21-6425 0840; e-mail: jianhexu@ecust.edu.cn or chunxiuli@ecust.edu.cn

[b] Shanghai Collaborative Innovation Centre for Biomanufacturing, School of Biotechnology, East China University of Science and Technology, 130 Meilong Road, Shanghai 200237, P. R. China

[c] Suzhou Bioforany EnzyTech Co. Ltd., No. 8 Yanjiuyuan Road, Economic Development Zone, Changshu, Jiangsu 215512, P. R. China

[#] These authors contributed equally to this work.

Received: ((will be filled in by the editorial staff))

Supporting information for this article is available on the WWW under http://dx.doi.org/10.1002/adsc.201######.((Please delete if not appropriate))

Abstract: 12α-Hydroxysteroid dehydrogenase (12α-HSDH) has the potential to convert cheap and readily available cholic acid (CA) to 12-oxochenodeoxycholic acid (12-oxo-CDCA), a key precursor for chemoenzymatic synthesis of the therapeutic bile acid ursodeoxycholic acid (UDCA). In this work, a native nicotinamide adenine dinucleotide (NAD^+)-dependent 12α-hydroxysteroid dehydrogenase (*Rr*12α-HSDH) from *Rhodococcus ruber* was identified using a structure-guided genome mining (SSGM) approach, which is based on the structure of cofactor pocket and the conserved nicotinamide cofactor binding motif alignment. *Rr*12α-HSDH was heterologously overexpressed in *Escherichia coli* BL21 (DE3), purified and characterized. The purified *Rr*12α-HSDH showed a high oxidative activity of 290 U $mg^{-1}_{protein}$ toward CA, with a catalytic efficiency (k_{cat}/K_M) of 5.10×10^3 mM^{-1} s^{-1}. In a preparative biotransformation (100 mL), CA (200 mM, 80 g L^{-1}) was efficiently converted to 12-oxo-CDCA in 1 h, with a 85% isolated yield and a space-time yield (STY) of up to 1632 g L^{-1} d^{-1}. Furthermore, *Rr*12α-HSDH was shown to be able to catalyze the oxidation of other 12α-hydroxysteroids at high substrate loads (up to 200 mM), giving the corresponding 12-oxo-hydroxysteroids in 71%−85% yields, indicating the great potential of *Rr*12α-HSDH as a promising biocatalyst for the synthesis of various therapeutic bile acids.

Keywords: biocatalysis; 12α-hydroxysteroid dehydrogenase; NAD^+-dependence; structure-guided genome mining; 12-oxochenodeoxycholic acid

Ursodeoxycholic acid (UDCA, **1e**, Scheme 1) is an active pharmaceutical ingredient of bear bile powder, which is a traditional Chinese medicine used for thousands of years.[1] Clinically, **1e** is an effective drug for the treatment of cholesterol gallstones and cholestatic diseases.[2] Traditionally, **1e** is either obtained from bear bile powder or produced chemically from cholic acid (CA, **1a**, Scheme 1), which is the most abundant and cheapest bile acid.[1,3] However, on the one hand, it is inhuman and unsustainable to extract **1e** from the bile of live bears. On the other hand, chemical synthesis requires multiple protection and deprotection steps, leading to a low/moderate overall yield (about 30%–53%), and the inevitable use of toxic and hazardous reagents (e.g., pyridine and CrO_3) generates copious amounts of waste.[4] Therefore, it is much more sustainable and economical enzymatic synthesis of **1e** from **1a**, given the availability of **1a** as a cheap raw material and the eco-friendly nature of the enzymatic reaction conditions.[3]

The enzymatic synthesis of **1e** requires the use of a very important class of enzymes, hydroxysteroid dehydrogenases (HSDHs), which can perform oxidoreduction of the hydroxyl/carbonyl groups on the core structure of hydroxysteroids.[5] These enzymes show very high regioselectivity toward the hydroxyl groups at different positions (e.g., C3, C7, and C12) of the steroid nucleus (Scheme 1).[3] Furthermore, HSDHs display excellent stereoselectivity for each of these positions by oxidizing hydroxyl groups oriented either below (α-OH) or above (β-OH) the plane of the steroid molecule.[6] To date, many HSDHs with known protein sequences have been reported. These include

3α-HSDHs from rat liver, *Comamonas testosteroni*, and *Eggerthella lenta*;[7] 7α-HSDHs from *Escherichia coli* HB101, *Eubacterium* sp. VPI 12708, *Clostridium sordelli*, *Bacteroides fragilis*, *Clostridium absonum* (formerly *Clostridium sardiniense*), *Clostridium difficile*, *Stenotrophomonas maltophilia*, and *Brevundimonas* sp.;[8] and 7β-HSDHs from *Collinsella aerofaciens*,[9a] *Clostridium absonum*,[8e] *Ruminococcus gnavus*,[9b] *Ruminococcus torques*,[9c] *Lactobacillus spicheri*,[8g] and *Clostridium* sp. Marseille.[8h] However, 12α-HSDHs with known gene sequences are rarely reported.[10]

12α-Hydroxysteroid dehydrogenase (12α-HSDH; EC 1.1.1.176) is a key enzyme for chemoenzymatic synthesis of **1e** from **1a**.[6] 12α-HSDHs catalyze the oxidation of the 12α-hydroxyl group of **1a**, forming 12-oxochenodeoxycholic acid (12-oxo-CDCA, **1b**), which can be subjected to a Wolff-Kishner-Huang reduction to remove the C12 carbonyl group. The 7α-hydroxylated chenodeoxycholic acid (CDCA, **1c**) is then epimerized to 7β-hydroxylated **1e** through the stable intermediate 7-oxo-lithocholic acid (7-oxo-LCA, **1d**) using two stereo-complementary enzymes, 7α-HSDH and 7β-HSDH (Scheme 1).[6,11] Up to now, the nicotinamide adenine dinucleotide phosphate ($NADP^+$)-dependent 12α-HSDH with published sequence was identified from *Clostridium* sp. strain ATCC 29733/VPI C48-50 and showed low catalytic activity.[7c,12] Ridlon *et al*. discovered several new 12α-HSDHs from *Eggerthella* sp. CAG:298, *Clostridium hylemonae*, *Clostridium scindens*, and *Clostridium hiranonis*, respectively.[7c,10]

Nevertheless, all of these documented 12α-HSDHs are stringently $NADP^+$-dependent oxidoreductases (Table 1, entries 3−7). When compared with $NADP^+$, nicotinamide adenine dinucleotide (NAD^+) is much less costly and more stable under industrial conditions, making it the preferred cofactor for practical application of dehydrogenases.[13] Most recently, a new NAD^+-dependent 12α-HSDH from *Eggerthella lenta* (*El*12α-HSDH) was reported by the group of Ulf Hanefeld. However, *El*12α-HSDH showed a productivity of only 4 g L^{-1} d^{-1} as a biocatalyst for the synthetic application.[14] Therefore, the identification of novel NAD^+-dependent 12α-HSDHs with high enzymatic activity for efficient and economical synthesis of **1e** precursor will promote sustainable and cost-efficient production of therapeutic bile acids.

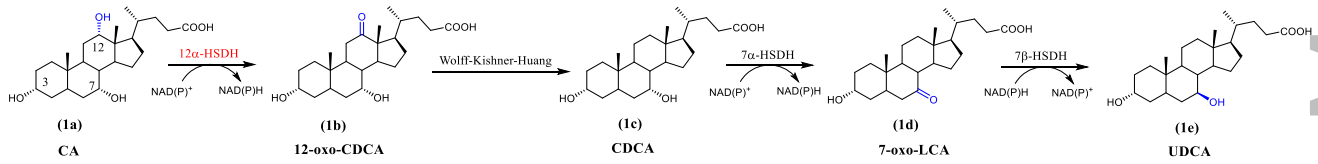

Scheme 1. 12α-HSDH mediated oxidation of **1a** as the first step of chemoenzymatic synthesis of **1e**.

Table 1. Specific activity of 12α-HSDHs toward **1a**.[a]

Entry	Enzyme	NCBI accession no.	Sequence identity [%]	Cofactor dependence	Specific activity [U mg^{-1}]
1	*Rr*12α-HSDH	WP_026137560.1	100	NAD^+	289 ± 13
2	*El*12α-HSDH	WP_114518444.1	43	NAD^+	76 ± 2.1
3	*Cl*12α-HSDH	ERJ00208.1	42	$NADP^+$	40 ± 0.8
4	*Eg*12α-HSDH	CDD59475.1	39	$NADP^+$	59 ± 0.3
5	rCHYL	EEG75500.1	42	$NADP^+$	103 ± 3
6	rCSCI	EDS06338.1	41	$NADP^+$	84 ± 2
7	rCHIR	EEA85268.1	38	$NADP^+$	197 ± 4

[a] Specific activity of 12α-HSDHs was measured in 100 mM potassium phosphate, pH 8.0, containing 1.0 mM NAD^+ or $NADP^+$, and 2 mM substrate **1a** at 30°C using purified enzyme.

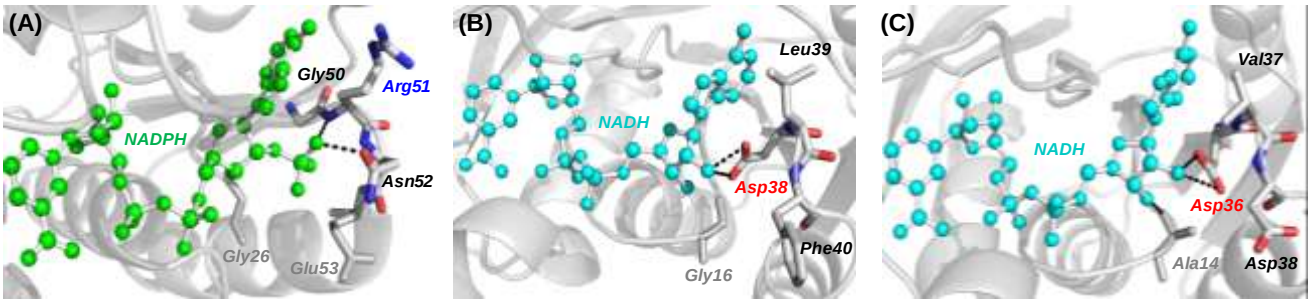

Figure 1. Structural models of (A) *Cl*12α-HSDH with NADPH, (B) *El*12α-HSDH with NADH, and (C) *Rr*12α-HSDH with NADH.

Herein, we discovered a new NAD^+-dependent *Rr*12α-HSDH (NCBI accession no. WP_026137560.1), which was identified from *Rhodococcus ruber* using a structure-guided genome mining (SGGM) approach based on the 3D structure of the enzyme's cofactor pocket and the alignment of a conserved nicotinamide cofactor-binding motif. *Rr*12α-HSDH possesses the highest specific activity toward **1a** when compared with other 12α-HSDHs (Table 1). Up to 200 mM (80 g L^{-1}) of **1a** was efficiently converted by *Rr*12α-HSDH to **1b** with a space-time yield (STY) of as high as 1632 g L^{-1} d^{-1} (Table 5, entry 7). Moreover, *Rr*12α-HSDH can bio-oxidize other 12*α*-bile acids and their glyco and tauro conjugates with 99% conversion, forming the corresponding 12-oxo-hydroxysteroids (Table 4), which are important precursors for the synthesis of pharmaceutically relevant bile acids.

To discover novel and native NAD^+-dependent 12α-HSDHs, a structure-guided genome mining (SGGM) strategy was proposed. Firstly, we structurally analyzed the phosphate- and hydroxyl-binding pockets of *Cl*12α-HSDH and *El*12α-HSDH, respectively. The phosphate-binding motif (GRN) in $NADP^+$-dependent *Cl*12α-HSDH (Figure 1A) was found to be replaced by a hydroxyl-binding motif (DLF) in the NAD^+-dependent *El*12α-HSDH (Figure 1B). This change in the amino acid residues located on the phosphate/hydroxyl-binding loops would be responsible for NAD(H)/NADP(H) cofactor recognition.[8g,14,15] In general, $NADP^+$-dependent enzymes have larger phosphate-binding pockets with positively charged residues (such as Arg51 in *Cl*12α-HSDH, Figure 1A) that interact with the negatively charged 2′-phosphate group of NADPH (phospho-) adenosine ribose, while NAD^+-dependent enzymes prefer negatively charged residues (such as Asp38 in *El*12α-HSDH, Figure 1B).[13c,15,16] Therefore, NAD^+-dependent enzymes could be rationally discovered by discriminating the residues on the cofactor pocket.

Subsequently, we performed a pBLAST search of the NCBI nonredundant database using the protein sequence of *El*12α-HSDH (NCBI accession no. WP_114518444.1) as the template, and carried out an alignment of the conserved cofactor-binding motifs. Twenty eight enzyme genes with negatively charged residues (Asp) on the *N*-terminal of hydroxyl-binding loop were selected from 1000 sequences (Figure S1), cloned into pET28a vector, and heterologously overexpressed in *Escherichia coli* BL21 (DE3) (Table S1). The activity of each enzyme (using crude enzyme extracts as the catalysts) toward **1a** was tested using NAD^+ as a cofactor. One of the tested enzymes, *Rr*12α-HSDH originating from *Rhodococcus ruber*, showed a significant activity on **1a** and was thus chosen for further studies. No activity was detected when using $NADP^+$ as a cofactor, indicating that *Rr*12α-HSDH is a native NAD^+-dependent enzyme. As shown in Figure 1C, a DVD motif was present on the hydroxyl-binding loop of the NAD^+-dependent *Rr*12α-HSDH. The negatively charged Asp36 residue may form hydrogen bonds with the 2′-hydroxyl group of the adenosine ribose in NADH, which facilitates the tight binding of NADH with the enzyme. However, this position in all the $NADP^+$-dependent 12α-HSDHs was replaced by a phosphate-binding motif (GRN) (Figure S6). The results demonstrated that SGGM strategy could enable effective and target-focused identification of the unknown but naturally occurring NAD^+-dependent dehydrogenases.

*Rr*12α-HSDH is shown to be a new 12α-HSDH because it shares only 38%–43% of its identity with the reported *El*12α-HSDH (*Eggerthella lenta*), *Cl*12α-HSDH (*Clostridium* sp. strain ATCC 29733/VPI C48-50), *Eg*12α-HSDH (*Eggerthella* sp. CAG: 298), rCHYL (*Clostridium hylemonae* DSM 15053), rCSCI (*Clostridium scindens* ATCC 35704), and rCHIR (*Clostridium hiranonis* DSM 13275) (Table 1). To characterize the enzymatic properties of *Rr*12α-HSDH, the *N*-terminal His-tagged recombinant enzyme was purified by nickel affinity chromatography and analyzed by sodium dodecyl sulfate polyacrylamide gel electrophoresis (Figure S2). As shown in Table 1, the oxidation activity of purified *Rr*12α-HSDH was 290 U $mg^{-1}_{protein}$ (under

standard conditions), which is the highest specific activity toward **1a** for 12α-HSDHs reported to date. *Rr*12α-HSDH showed higher catalytic activity at a temperature range of 35–45°C, and exhibited the highest activity at 40°C, retaining 70% activity at 30°C (Figure S3). The pH properties of the purified *Rr*12α-HSDH in both the reductive and oxidative reactions are shown in Figure S4. *Rr*12α-HSDH displayed a maximum activity at pH 10.0 for **1a** dehydrogenation with NAD^+ as a cofactor and an optimum at pH 6.0 for **1b** reduction with NADH as a cofactor. The thermostability of *Rr*12α-HSDH was also examined, giving half-lives ($t_{1/2}$) of 72, 20, and 0.25 h, respectively, at 30, 40, and 50°C (Figure S5), implying that the enzyme was quite stable at 30°C but deactivated at higher temperatures. Hence, the enzymatic synthesis reactions were performed at 30°C so as to avoid the negative influences of the poor thermostability.

The kinetic parameters of 12α-HSDHs toward **1a** and cofactor were determined. As shown in Table 2 (entries 1−2), the Michaelis−Menten constant (K_m) of *Rr*12α-HSDH for **1a** was 0.025 mM, displaying a 25-fold higher affinity than *El*12α-HSDH (0.64 mM). The turnover frequency (k_{cat}) of *Rr*12α-HSDH for **1a** was 128 s^{-1}, affording the catalytic efficiency (k_{cat}/K_m) of 5.10 × 10^3 mM^{-1} s^{-1}, which is 88-fold greater than that of *El*12α-HSDH. In addition, compared with *El*12α-HSDH, *Rr*12α-HSDH showed a much better affinity to cofactor NAD^+ with a K_m of 0.063 mM (Table 2, entry 3), which is 15 times lower than *El*12α-HSDH (0.92 mM) (Table 2, entry 4), indicating that *Rr*12α-HSDH has a greater application prospect in enzymatic synthesis. The kinetic parameters of *Rr*12α-HSDH toward other 12α-hydroxysteroids were also measured, as summarized in Table 2 (entries 5−11). *Rr*12α-HSDH exhibited relatively high k_{cat} values for all the 12α-hydroxysteroids tested (78.3–141 s^{-1}) and the highest k_{cat} was observed when using glycocholic acid (GCA, **6a**) as substrate. The K_m values of *Rr*12α-HSDH for majority of the 12α-hydroxysteroids ranged from 0.025 to 0.046 mM, indicating that the enzyme has excellent affinity to these substrates except for deoxycholic acid (DCA, **4a**, K_m = 0.138 mM). The results demonstrated that *Rr*12α-HSDH can be used as a potential biocatalyst for the production of various health-promoting bile acids.

Table 2. Kinetic parameters of recombinant *Rr*12α-HSDH and *El*12α-HSDH.[a]

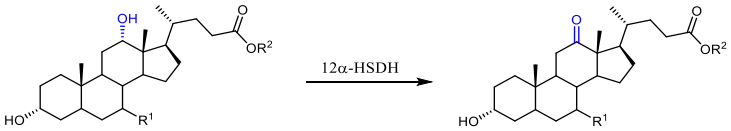

1a–8a **1b–8b**

Entry	Substrate (R^1 =, R^2 =)	V_{max} [μmol·min^{-1}·mg^{-1}]	K_m [mM]	k_{cat} [s^{-1}]	k_{cat}/K_m [mM^{-1} s^{-1}]
1	**1a** (α-OH, H)	290 ± 13	0.025 ± 0.005	128 ± 6	5.10 × 10^3
2	**1a** (α-OH, H)[b]	78 ± 2.1	0.640 ± 0.060	36.5 ± 1.0	57.0
3	NAD^+[c]	292 ± 5	0.063 ± 0.005	129 ± 2	2.03 × 10^3
4	NAD^+[d]	65 ± 6	0.920 ± 0.160	30.6 ± 2.6	33.3
5	**2a** (Ketone, H)	178 ± 4	0.041 ± 0.003	78.3 ± 1.8	1.91 × 10^3
6	**3a** (β-OH, H)	240 ± 13	0.046 ± 0.008	106 ± 6	2.30 × 10^3
7	**4a** (H, H)	276 ± 21	0.138 ± 0.003	121 ± 9	8.80 × 10^2
8	**5a** (α-OH, Taurine)	319 ± 15	0.035 ± 0.007	140 ± 7	4.01 × 10^3
9	**6a** (α-OH, Glycine)	320 ± 15	0.042 ± 0.008	141 ± 7	3.35 × 10^3
10	**7a** (H, Taurine)	295 ± 8	0.038 ± 0.004	130 ± 4	3.40 × 10^3
11	**8a** (H, Glycine)	293 ± 4	0.042 ± 0.002	129 ± 2	3.10 × 10^3

[a] Kinetic parameters were determined at different substrate concentrations (0–10 mM) in the presence of 1 mM NAD^+ using purified *Rr*12α-HSDH, and [b] *El*12α-HSDH, respectively. [c] Kinetic parameters were determined at different NAD^+ concentrations (0–1.0 mM) in the presence of 2 mM **1a** using purified *Rr*12α-HSDH, and [d] *El*12α-HSDH, respectively. The k_{cat} values were calculated considering a subunit size of 28.0 and 28.3 kDa for *Rr*12α-HSDH and *El*12α-HSDH, respectively.

Table 3. Optimization of reaction conditions for the oxidation of **1a** catalyzed by *Rr*12α-HSDH.[a]

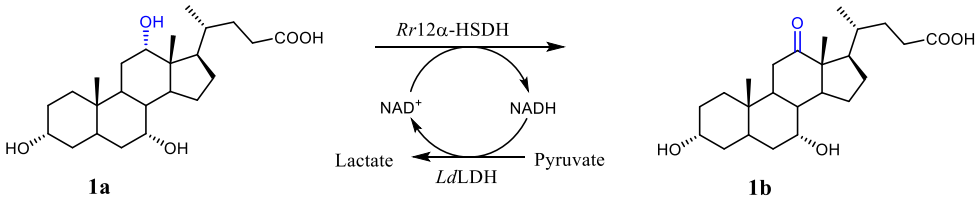

Entry	**1a** [mM]	*Rr*12α-HSDH [g L^{-1}]	NAD^+ [mM]	Time [h]	Conv. [%][b]
1	50	1	0.2	0.5	>99
2	100	1	0.2	24	82
3	100	1	0.4	1	>99
4	200	2	0.4	12	50
5	200	2	0.6	1.5	>99
6	200	5	0.5	0.5	>99

[a] Reaction conditions: 10 mL reaction mixture, containing 50–200 mM substrate **1a**, 1.5-fold equivalent pyruvate, 1–5 g L^{-1} each of lyophilized *E. coli* cells harboring *Rr*12α-HSDH and *Ld*LDH genes respectively, 0.2–0.6 mM NAD^+, and potassium phosphate buffer (100 mM, pH 8.0), was incubated at 30°C and 220 rpm. [b] Conversion was determined by reversed-phase high-performance liquid chromatography (RP-HPLC).

To evaluate the feasibility of utilizing *Rr*12α-HSDH for the biocatalytic process, the pyruvate/LDH system was chosen for the regeneration of cofactor NAD^+. Compared with other NAD^+ regeneration systems such as O_2/NOX and α-ketoglutarate/glutamate dehydrogenase system, the lactate dehydrogenase (*Ld*LDH) identified from *Lactobacillus delbrueckii subsp. bulgaricus Ld*LDH possesses higher specific activity (331 U $mg^{-1}_{protein}$).[11a,17a] In practical industrial applications, the supply of O_2 could be very problematic,[17b] and α-ketoglutarate is very expensive since it is used for medical treatments and as a chemical building block.[17c] The pyruvate/LDH system utilized to regenerate cofactor NAD^+ is more efficient and economical. Initial experiments were performed in a 10 mL reaction system with 50 mM **1a**, 0.2 mM NAD^+, 75 mM pyruvate, and 1 g L^{-1} each of lyophilized *E. coli* cells harboring *Rr*12α-HSDH and *Ld*LDH genes, respectively. As a result, **1a** was completely converted to **1b** within 0.5 h (Table 3, entry 1). An increase of substrate loading to 100 mM without changing other conditions led to 82% conversion in 24 h (Table 3, entry 2). When 0.4 mM NAD^+ was added to the reaction mixture, *Rr*12α-HSDH completely oxidized 100 mM **1a** within 1 h (Table 3, entry 3). The substrate loading could be further raised to 200 mM, but the conversion was only 50% after 12 h (Table 3, entry 4). It was found that 99% conversion could be achieved in 1.5 h with a load of 0.6 mM cofactor (Table 3, entry 5). For cost effectiveness, taking into account the internal cofactor content of lyophilized *E. coli* cells,[18] the reaction was carried out using 5 g L^{-1} biocatalyst and 0.5 mM of external NAD^+. Accordingly, 200 mM substrate was transformed completely with 99% conversion within 0.5 h (Table 3, entry 6), indicating the great potential of *Rr*12α-HSDH as a biocatalyst for practical applications. In the 10-mL scale biotransformation, 50 mM CA could be rapidly converted to 12-oxo-CDCA. But when the substrate loading was gradually increased to 200 mM, both the concentrations of biocatalyst and cofactor had to be increased simultaneously to achieve complete oxidation of CA, indicating that the enzymes and cofactor might have been partially inactivated during the reaction. Further work will be required to elucidate the mechanisms that lead to the loss of enzyme activity and/or degradation of the cofactor.

Finally, in order to demonstrate the practical capability of *Rr*12α-HSDH for synthetic reactions, the oxidation of various 12α-hydroxysteroids were performed on a preparative scale (100 mL) under the optimized conditions. Consequently, 200 mM **1a** was completely oxidized (>99% conversion) into **1b** by *Rr*12α-HSDH within 1 h. After extraction and purification, **1b** was isolated in 85% yield (Table 4, entry 1), giving a STY of up to 1632 g L^{-1} d^{-1}, which represents the highest reported productivity to the best of our knowledge (Table 5). For substrates 7-

oxo-deoxycholic acid (7-oxo-DCA, **2a**), ursocholic acid (UCA, **3a**), and **4a**, the corresponding products 7,12-dioxo-lithocholic acid (7,12-dioxo-LCA, **2b**), 12-oxoursodeoxycholic acid (12-oxo-UDCA, **3b**), and 12-oxo-lithocholic acid (12-oxo-LCA, **4b**) were isolated after 3.5−4.5 h of reaction in 75%, 81%, and 82% yields, respectively, albeit at a slightly lower substrate loading (150 mM) (Table 4, entries 2−4). Their respective STYs, 240, 333, and 295 g L^{-1} d^{-1}, were obviously lower than that of **1b**. This might be attributed to the slightly lower k_{cat} of *Rr*12α-HSDH toward **2a** and **3a** and higher K_m toward **4a** than **1a** (Table 2, entries 5−7). Following the same protocol, 200 mM substrates of taurocholic acid (TCA, **5a**), glycocholic acid (GCA, **6a**), taurodeoxycholic acid (TDCA, **7a**), and glycodeoxycholic acid (GDCA, **8a**) were totally converted within 1−2 h, affording the corresponding 12-oxo-hydroxysteroids with 99% conversion (Table 4, entries 5−8). These results demonstrated that *Rr*12α-HSDH is an efficient biocatalyst for the technically competitive and economically viable bioproduction of 12-oxo-hydroxysteroids, all acting as precursors for manufactory of therapeutic bile acids.

Table 4. Oxidation of hydroxysteroids catalyzed by *Rr*12α-HSDH.[a]

Entry	Substrate	Product	Substrate load [mM]	Time [h]	Conv.[b] /Yield[c] [%]
1	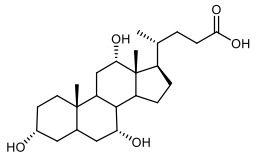 **1a**	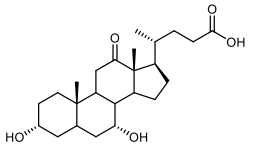 **1b**	200	1	>99/85
2	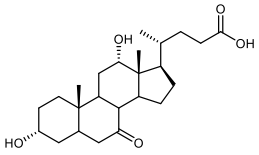 **2a**	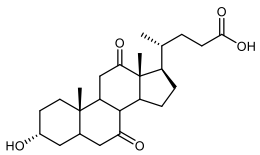 **2b**	150	4.5	>99/75
3	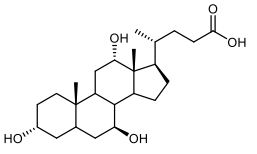 **3a**	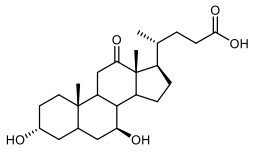 **3b**	150	3.5	>99/81
4	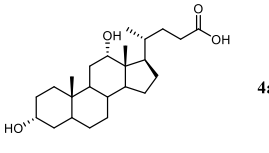 **4a**	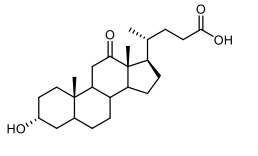 **4b**	150	4	>99/82
5	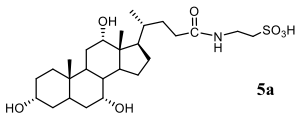 **5a**	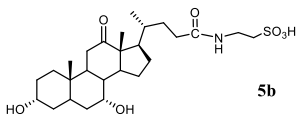 **5b**	200	1.5	>99
6	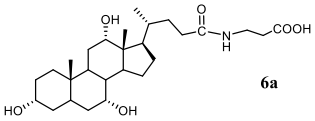 **6a**	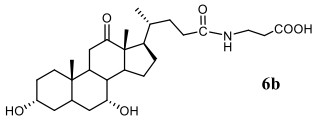 **6b**	200	1	>99
7	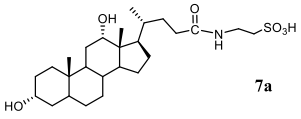 **7a**	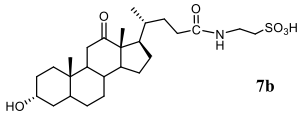 **7b**	200	1.5	>99
8	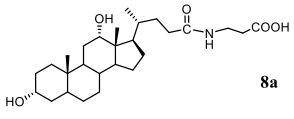 **8a**	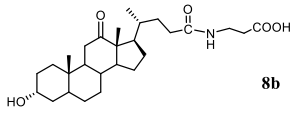 **8b**	200	2	>99

[a] Reaction conditions: 100 mL reaction mixture, containing 150−200 mM substrate, 1.5-fold equivalent pyruvate, 5 g L^{-1} lyophilized *E. coli* cell harboring *Rr*12α-HSDH gene, 5 g L^{-1} lyophilized *E. coli* cell harboring *Ld*LDH gene, 0.5 mM NAD^+, and potassium phosphate buffer (100 mM, pH 8.0), was incubated at 30°C and 220 rpm. [b] Conversion was determined by RP-HPLC. [c] Isolated yields.

Table 5. Comparison of *Rr*12α-HSDH with other reported catalysts in synthesis of **1b** from **1a**.

Entry	Catalyst	**1a** [mM]	Time [h]	Conv. /Yield [%]	*E* factor[a]	Atom efficiency [%][b]	STY [g L^{-1} d^{-1}]	Ref.
1	Chemical catalysts[c]	312.5	21	47.5	55.4	48.5	68	Hofmann[4]
2	12α-HSDH[d]	100	4	>99/88	1.8	64.3	240	Carrea et al.[19]
3	12α-HSDH[e]	100	24	92	6.1	87.1	37	Fossati et al.[20]
4	12α-HSDH[f]	12	12	98	3.3	81.9	9	Giovannini et al.[21]
5	*El*12α-HSDH[g]	10	24	>99	2.5	95.8	4	Tonin et al.[14]
6	*El*12α-HSDH[h]	10	4	>99	4.4	75.2	24	Tonin et al.[14]
7	*Rr*12α-HSDH[i]	200	1	>99/85	1.08	81.9	1632	This work

[a] The calculations did not take into account the waste generated for the preparation of the catalysts and the downstream processes. The detailed calculations of *E* factor and [b] atom efficiency are listed in Supporting Information. [c] The 400 mL reaction mixture contained 50 g **1a** (312.5 mM). [d] 12α-HSDH was extracted from *Clostridium* group P. 70 mL reaction mixture contained 0.37 U/mL 12α-HSDH and 0.06 mM $NADP^+$. [e] Purified 12α-HSDH from *Clostridium* sp. 10 mL reaction mixture contained 20 U/mL 12α-HSDH and 0.1 mM $NADP^+$. [f] Partially purified 12α-HSDH from *calcoaceticus lwoffii*. 100 mL reaction mixture contained 0.028 U/mL 12α-HSDH and 0.2 mM NAD^+. [g] Purified *El*12α-HSDH (recombinant *E. coli*/pET28a-*El*12α-HSDH) combined with NOX (75 mL reaction mixture contained 0.1 U/mL *El*12α-HSDH and 0.5 mM NAD^+), and [h] MDH (50 mL reaction mixture contained 0.1 U/mL *El*12α-HSDH and 0.5 mM NAD^+), respectively. [i] Lyophilized cells of recombinant *E. coli*/pET28a-*Rr*12α-HSDH. 100 mL reaction mixture contained 10 U/mL *Rr*12α-HSDH and 0.5 mM NAD^+.

The enzymatic synthesis of **1b** from **1a** mediated by the combination of *Rr*12α-HSDH and LDH showed an atom efficiency of 81.9% (Table 5), slightly lower than that obtained by the *El*12α-HSDH combined with NOX, but still acceptable compared with the chemical route. More importantly, as shown in Table 5, the *E* factor (environmental factor) for the production of **1b** catalyzed by *Rr*12α-HSDH was estimated to be 1.08, in contrast to those for other reported biocatalysts and 55.4 for the chemical route, indicating the significant environmental benefit of biocatalysts, especially *Rr*12α-HSDH.

In summary, a new and native NAD^+-dependent *Rr*12α-HSDH with high catalytic efficiency was discovered from *Rhodococcus ruber* by the proposed structure-guided genome mining approach (SGGM). *Rr*12*α*-HSDH showed higher specific activity toward **1a** than other reported 12α-HSDHs. By stepwise optimization of reaction conditions, as much as 80 g L^{-1} (200 mM) of **1a** could be completely oxidized within 1 h, and efficiently converted to **1b**, with an isolated yield of 85% and a STY of up to 1632 g L^{-1} d^{-1}. The biocatalytic process gave an atom efficiency of 81.9% and an *E* factor of 1.08. Furthermore, various 12α-hydroxysteroids were bio-oxidized to the corresponding 12-oxo-hydroxysteroids by *Rr*12α-HSDH at high substrate loads (up to 200 mM) and in good yields (up to 85%), indicating that *E. coli*/pET28a-*Rr*12α-HSDH can serve as an attractive biocatalyst for highly efficient and environmentally benign production of important scaffolds of pharmaceutical bile acids. Further reaction engineering for pilot-scale and large-scale applications is ongoing in our laboratory.

Experimental Section

Structure-Guided Genome Mining of New 12α-HSDHs

To discover novel and native NAD^+-dependent 12*α*-HSDHs, a structure-guided genome mining (SGGM) strategy was adopted. We performed a pBLAST search of the NCBI nonredundant database (http://www.ncbi.nlm.nih.gov) using the protein sequence of *El*12α-HSDH (NCBI accession no. WP_114518444.1) as the template, and carried out an alignment of the conserved cofactor-binding motifs. To ensure the diversity of sequences, 1000 candidate sequences with 20−60% similarities to the template sequence were selected. Based on the fact that the residues located on the phosphate/hydroxyl-binding loops would be responsible for NAD(H)/NADP(H) cofactor recognition, 28 putative 12α-HSDH sequences encoding a negatively charged amino acid residue (Asp) on the *N*-terminal of hydroxyl-binding loop were chosen among the 1000 candidate genes and used for cloning, expression, and activity detection (Supporting Information).

Activity Assays and Kinetic Parameters

Enzyme activity was determined by spectrophotometric assay at 30°C measuring the oxidation of NAD(P)H or reduction of $NAD(P)^+$ at 340 nm (ε = 6.22 mM^{-1} cm^{-1}). The reaction mixture (1 mL) was composed of 970 μL potassium phosphate buffer (KPi, 100 mM, pH 8.0), 10 μL of substrate stock solution (200 mM), 10 μL NAD(H) or NADP(H) solution (100 mM), and 10 μL purified enzyme with an appropriate concentration. One unit of the enzyme activity is defined as the amount of enzyme that catalyzes the reduction (or oxidation) of 1 μmol NAD(P)(H) per minute under the assay conditions. Kinetic parameters were determined at different substrate concentrations (0–10 mM) and cofactor (NAD^+ or $NADP^+$) concentrations (0–1.0 mM). The resultant data were adjusted to a Michaelis-Menten model using Origin 8.6.

Preparative Synthesis of 12-Oxo-hydroxysteroids

The biotransformation was conducted at 30°C and 220 rpm for 24 h in a 100 mL solution containing 150–200 mM 12α-hydroxysteroids, 1.5-fold equivalent pyruvate, 5 g L^{-1} each of lyophilized *E. coli* cells harboring *Rr*12*α*-HSDH and *Ld*LDH genes respectively, 0.5 mM NAD^+, and potassium phosphate buffer (KPi, 100 mM, pH 8.0). The conversion of substrates was determined by RP-HPLC (Supporting Information). After complete conversion, the solution was acidified with 1 M HCl till pH 3.0, and the precipitated product was filtered and washed with 50−100 mL of ethanol. Subsequently, the ethanol is evaporated, and the powder was dried, and purified by silica gel column chromatography eluting with a mixture of dichloromethane and methanol (20/1–10/1) to yield pure 12-oxo-hydroxysteroids. The product was characterized by NMR spectroscopy and high-resolution mass spectrometry (HRMS) (Supporting Information).

Acknowledgements

This work was financially supported by The National Key Research and Development Program of China (No. 2018YFC1706200), The National Natural Science Foundation of China (Nos. 21536004, 21871085, and 31500592), and the Fundamental Research Funds for the Central Universities (No. 22221818014). We are grateful to Dr. Yu-Cong Zheng and Dr. Chao Shou, both from East China University of Science and Technology, for their experimental assistance.

References

[1] Y. Feng, K. Siu, N. Wang, K. M. Ng, S. W. Tsao, T. Nagamatsu, Y. Tong, *J. Ethnobiol. Ethnomed.* **2009**, *5*, 2.

[2] T. Ikegami, Y. Matsuzaki, *Hepatol. Res.* **2008**, *38*, 123–131.

[3] a) F. Tonin, I. W. C. E. Arends, *Beilstein J. Org. Chem.* **2018**, *14*, 470–483; b) T. Eggert, D. Bakonyi, W. Hummel, *J. Biotechnol.* **2014**, *191*, 11–21.

[4] a) A. F. Hofmann, *Acta Chem. Scand.* **1963**, *17*, 173–186; b) P. S. Dangate, C. L. Salunke, K. G. Akamanchi, *Steroids* **2011**, *76*, 1397–1399.

[5] a) S. Savino, E. E. Ferrandi, F. Forneris, S. Rovida, S. Riva, D. Monti, A. Mattevi, *Proteins Struct. Funct. Bioinf.* **2016**, *84*, 859–865. b) R. Wang, J. Wu, D. K. Jin, Y. Chen, Z. Lv, Q. Chen, Q. Miao, X. Huo, F. Wang, *Acta Crystallogr., Sect. F: Struct. Biol. Cryst. Commun.* **2017**, *73*, 246–252.

[6] D. Monti, E. E. Ferrandi, I. Zanellato, L. Hua, F. Polentini, G. Carrea, S. Riva, *Adv. Synth. Catal.* **2009**, *351*, 1303–1311.

[7] a) J. E. Pawlowski, M. Huizinga, T. M. Penning, *J. Biol. Chem.* **1991**, *266*, 8820–8825; b) C. Grimm, E. Maser, E. Möbus, G. Klebe, K. Reuter, R. Ficner, *J. Biol. Chem.* **2000**, *275*, 41333–41339; c) S. M. Mythen, S. Devendran, C. Méndez-García, I. Cann, J. M. Ridlon, *Appl. Environ. Microbiol.* **2018**, *84*, e02475-17.

[8] a) T. Yoshimoto, H. Higashi, A. Kanatani, X. S. Lin, H. Nagai, H. Oyama, K. Kurazono, D. Tsuru, *J. Bacteriol.* **1991**, *173*, 2173–2179; b) S. F. Baron, C. V. Franklund, P. B. Hylemon, *J. Bacteriol.* **1991**, *173*, 4558–4569; c) J. P. Coleman, L. L. Hudson, M. J. Adams, *J. Bacteriol.* **1994**, *176*, 4865–4874; d) M. J. Bennett, S. L. McKnight, J. P. Coleman, *Curr. Microbiol.* **2003**, *47*, 475–484; e) E. E. Ferrandi, G. M. Bertolesi, F. Polentini, A. Negri, S. Riva, D. Monti, *Appl. Microbiol. Biotechnol.* **2012**, *95*, 1221–1233; f) D. Bakonyi, W. Hummel, *Enzyme Microb. Technol.* **2017**, *99*, 16–24; g) F. Tonin, L. G. Otten, I. W. C. E. Arends, *ChemSusChem* **2019**, *12*, 3192–3203; h) X. Chen, Y. Cui, J. Feng, Y. Wang, X. Liu, Q. Wu, D. Zhu, Y. Ma, *Adv. Synth. Catal.* **2019**, *361*, 2497–2504.

[9] a) L. Liu, A. Aigner, R. D. Schmid, *Appl. Microbiol. Biotechnol.* **2011**, *90*, 127–135; b) J. Y. Lee, H. Arai, Y. Nakamura, S. Fukiya, M. Wada, A. Yokota, *J. Lipid Res.* **2013**, *54*, 3062–3069; c) M. M. Zheng, R. F. Wang, C. X. Li, J. H. Xu, *Process Biochem.* **2015**, *50*, 598–604.

[10] H. Doden, L. A. Sallarn, S. Devendran, L. Ly, G. Doden, S. L. Daniel, J. M. P. Alves, J. M. Ridlon, *Appl. Environ. Microbiol.* **2018**, *84*, e00235-18.

[11] a) M. M. Zheng, K. C. Chen, R. F. Wang, H. Li, C. X. Li, J. H. Xu, *J. Agric. Food. Chem.* **2017**, *65*, 1178–1185; b) M. Braun, B. Sun, B. Anselment, D. Weuster-Botz, *Appl. Microbiol. Biotechnol.* **2012**, *95*, 1457–1468; c) D. Bakonyi, A. Wirtz, W. Hummel, *Z. Naturforsch.* **2012**, *67*, 1037–1044; d) L. Liu, M. Braun, G. Gebhardt, D. Weuster-Botz, R. Gross, R. D. Schmid, *Appl. Microbiol. Biotechnol.* **2013**, *97*, 633–639; e) B. Sun, C. Kantzow, S. Bresch, K. Castiglione, D. Weuster- Botz, *Biotechnol. Bioeng.* **2013**, *110*, 68–77; f) B. Sun, F. Hartl, K. Castiglione, D. Weuster- Botz, *Biotechnol. Progr.* **2015**, *31*, 375–386.

[12] M. Braun, H. Link, L. Liu, R. D. Schmid, Weuster- Botz, D. *Biotechnol. Bioeng.* **2011**, *108*, 1307–1317.

[13] a) C. You, R. Huang, X. L. Wei, Z. G. Zhu, Y. H. P. Zhang, *Synth. Syst. Biotechnol.* **2017**, *2*, 208–218; b) P. M. Thompson, N. J. Turner, *ChemCatChem* **2017**, 9, 3833–3836; c) J. K. B. Cahn, C. A. Werlang, A. Baumschlager, S. Brinkmann-Chen, S. L. Mayo, F. H. Arnold, *ACS Synth. Biol.* **2017**, *6*, 326–333; d) A. M. Chánique, L. P. Parra, *Front. Microbiol.* **2018**, *9*, 194.

[14] F. Tonin, N. Alvarenga, J. Z. Ye, I. W. C. E. Arends, U. Hanefeld, *Adv. Synth. Catal.* **2019**, *361*, 2448–2455.

[15] Z. N. You, Q. Chen, S. C. Shi, M. M. Zheng, J. Pan, X. L. Qian, C. X. Li, J. H. Xu, *ACS Catal.* **2019**, *9*, 466–473.

[16] a) N. S. Scrutton, A. Berry, R. N. Perham, *Nature* **1990**, *343*, 38–43; b) A. Lerchner, A. Jarasch, W. Meining, A. Schiefner, A. Skerra, *Biotechnol. Bioeng.* **2013**, *110*, 2803–2814.

[17] a) S. Kochhar, N. Chuard, H. Hottinger, *J. Biol. Chem.* **1992**, *267*, 20298–20301. b) F. Sha, Y. Zheng, J. Chen, K. Chen, F. Cao, M. Yan, P. Ouyang, *Green Chem.* **2018**, *20*, 2382–2391. c) B. Beer, A. Pick, V. Sieber, *Metab. Eng.* **2017**, *40*, 5–13.

[18] a) Q. Li, B. Huang, Q. He, J. Lu, X. Li, Z. Li, H. Wu, Q. Ye, *Bioresour. Bioprocess.* **2018**, *5*, 41. b) M. S. Rahman, C. C. Xu, W. Qin, *Bioresour. Bioprocess.* **2018**, *5*, 3. c) K. Y. San, G. N. Bennett, S. J. Berríos-Rivera, Vadali, R. V.; Y. T. Yang, E. Horton, F. B. Rudolph, B. Sariyar, K. Blackwood, *Metab. Eng.* **2002**, *4*, 182–192.

[19] G. Carrea, R. Bovara, R. Longhi, S. Riva, *Enzyme Microb. Technol.* **1985**, *7*, 597–600.

[20] E. Fossati, F. Polentini, G. Carrea, S. Riva, *Biotechnol. Bioeng.* **2006**, *93*, 1216–1220.

[21] P. P. Giovannini, A. Grandini, D. Perrone, P. Pedrini, G. Fantin, M. Fogagnolo, *steroids* **2008**, *73*, 1385–1390.

10.1002/adsc.201900849

COMMUNICATION

Efficient Synthesis of 12-Oxochenodeoxycholic Acid Using a 12α-Hydroxysteroid Dehydrogenase from *Rhodococcus ruber*

Adv. Synth. Catal. **Year**, *Volume*, Page – Page

Shou-Cheng Shi,[+a] Zhi-Neng You,[+a] Ke Zhou,[a] Qi Chen,[a, b] Jiang Pan,[a, b] Xiao-Long Qian,[c] Jian-He Xu,[a, b,*] and Chun-Xiu Li[a, b,*]